Peroxygenase-Catalysed Selective Oxidation of Silanes to Silanols

Xu, Xiaomin; van Hengst, Jacob M.A.; Mao, Yejia; Martinez, Mireia; Roda, Sergi; Floor, Martin; Guallar, Victor; Paul, Caroline E.; Alcalde, Miguel; Hollmann, Frank

DOI
10.1002/anie.202302844

Publication date
2023

Document Version
Final published version

Published in
Angewandte Chemie - International Edition

Biocatalysis

How to cite:
International Edition: doi.org/10.1002/anie.202302844
German Edition: doi.org/10.1002/ange.202302844

Peroxygenase-Catalysed Selective Oxidation of Silanes to Silanols

*Xiaomin Xu[+], Jacob M. A. van Hengst[+], Yejia Mao, Mireia Martinez, Sergi Roda, Martin Floor, Victor Guallar, Caroline E. Paul, Miguel Alcalde, and Frank Hollmann**

Abstract: A peroxygenase-catalysed hydroxylation of organosilanes is reported. The recombinant peroxygenase from *Agrocybe aegerita* (*Aae*UPO) enabled efficient conversion of a broad range of silane starting materials in attractive productivities (up to 300 mM h^{-1}), catalyst performance (up to 84 s^{-1} and more than 120000 catalytic turnovers). Molecular modelling of the enzyme-substrate interaction puts a basis for the mechanistic understanding of *Aae*UPO selectivity.

Silanols represent an important product class in organic chemistry as precursors for silicones, as catalyst components or in medicinal chemistry.[1] Syntheses of the state-of-the-art typically start from already functionalised silanes such as chloro- or alkoxysilanes via hydrolysis and producing significant amounts of salt waste-products (Scheme 1a).[1b,2] Less waste-intensive methods involving dehydrogenative,[3] O_2[4] or H_2O_2[5]-dependent oxidation of non-functionalised silanols are rare (Scheme 1b,c). Even less common are biocatalytic methods for the conversion of silanes,[6] even though in the past years a rich hydrolase-catalysed silanol chemistry has evolved.[7] Recently, Arnold and co-workers succeeded in evolving a cytochrome P450 BM3 variant which dramatically increased catalytic activity towards a range of organosilanes (Scheme 1d).[6a]

Inspired by these pioneering works, we asked ourselves whether so-called unspecific peroxygenases (UPOs) may also

a) hydrolysis of chlorosilanes

$R_3Si\text{-}Cl + H_2O \longrightarrow R_3Si\text{-}OH + HCl$

b) dehydrogenative oxidation of silanes

$R_3Si\text{-}H + H_2O \xrightarrow{Cat} R_3Si\text{-}OH + H_2 + SiR_3\text{-}O\text{-}SiR_3$

c) oxygen-driven oxidations

$R_3Si\text{-}H + (H_2)O_2 \xrightarrow{Cat} R_3Si\text{-}OH + SiR_3\text{-}O\text{-}SiR_3 + H_2O$

d) P450 monooxygenase-catalysed oxidation of silanes

$R_3Si\text{-}H + NADPH + O_2 \xrightarrow{P450} R_3Si\text{-}OH + NADP^+ + H_2O$

e) this work: peroxygenase-catalysed oxidation of silanes

$R_3Si\text{-}H + H_2O_2 \xrightarrow{UPO} R_3Si\text{-}OH + H_2O$

Scheme 1. Synthetic accesses to silanols compared to the system proposed here.

be suitable catalysts for this type of transformation. Particularly, we investigated the UPO from *Agrocybe aegerita* (*Aae*UPO)[8] as silane oxyfunctionalisation catalyst. UPOs are attractive alternatives to established P450 monooxygenases as they enable drastically simplified, NAD(P)H-independent reactions using only H_2O_2 as stoichiometric oxidant (Scheme 1e).[9]

In a first experiment, we performed the H_2O_2-dependent hydroxylation of dimethylphenylsilane (**1a**) to the corresponding dimethylphenylsilanol (**2a**) catalysed by *Aae*UPO under otherwise identical conditions. Because of the poor water solubility of **1a**, 30 % (v/v) of acetonitrile was added, which was feasible due to the extraordinary solvent tolerance of *Aae*UPO.[10]

As *Aae*UPO, just as any heme-dependent enzyme, is irreversibly inactivated in the presence of high H_2O_2 concentrations,[11,12] we decided for a H_2O_2 feeding strategy to avoid accumulation of H_2O_2. Using 1 μM of *Aae*UPO and a H_2O_2 feeding rate of 10 mM h^{-1}, full conversion of the starting material was achieved within 5 h of reaction time, corresponding to an excellent total turnover number and turnover frequency for *Aae*UPO of 40000 and 2.2 s^{-1}, respectively (Figure 1). No by-product formation was observed. Control reactions in the absence of *Aae*UPO or using thermally inactivated *Aae*UPO did not yield detectable conversion of **1a** under otherwise identical conditions.

Next, we investigated the effect of H_2O_2 dosage on the rate and robustness of the *Aae*UPO-catalysed hydroxylation of **1a** (Figure 2). Up to a H_2O_2-addition rate of 500 mM h^{-1} the product formation rate almost linearly increased with increas-

[*] Dr. X. Xu,[+] Dr. J. M. A. van Hengst,[+] Y. Mao, Dr. C. E. Paul, Prof. Dr. F. Hollmann
Department of Biotechnology, Delft University of Technology
van der Maasweg 9, 2629HZ Delft (The Netherlands)
E-mail: f.hollmann@tudelft.nl
M. Martinez, S. Roda, Dr. M. Floor, Prof. V. Guallar
Department of Life Sciences, Barcelona Supercomputing Center
Plaza Eusebi Güell 1-3 08034Barcelona (Spain)
Prof. V. Guallar
Institució Catalana de Recerca i Estudis Avançats
Passeig de Lluís Companys, 23, 08010 Barcelona (Spain)
Prof. Dr. M. Alcalde
Department of Biocatalysis, Institute of Catalysis, CSIC
Madrid (Spain)
[+] These authors contributed equally to this work.

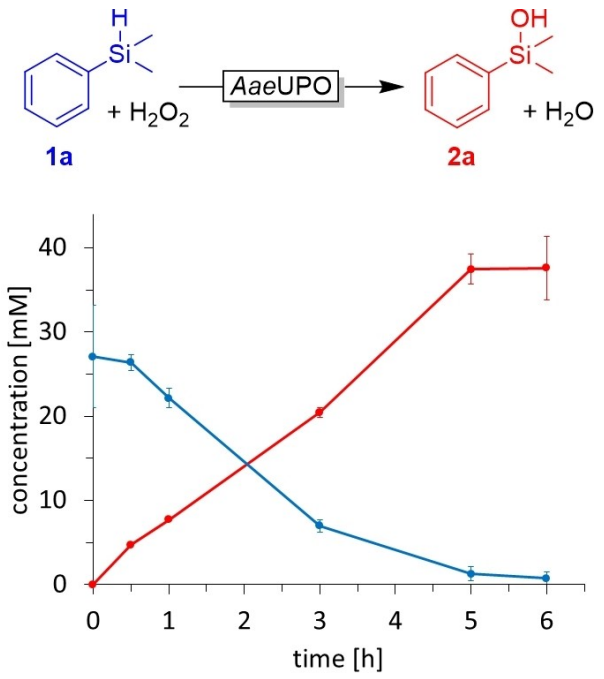

Figure 1. *Aae*UPO-catalysed hydroxylation of dimethylphenylsilane (**1a**) to dimethylphenylsilanol (**2a**). Conditions: [**1a**] = 50 mM, [*Aae*UPO] = 1 μM, buffer: 50 mM KPi pH 7.0 containing 30% (v/v) of acetonitrile, 25 °C, 600 rpm, H_2O_2 feeding-rate: 10 mM × h^{-1} (from a 1 M stock). Please note that even in the presence of 30% (v/v) of acetonitrile, the starting material was not fully soluble explaining the lower than nominal initial concentration of **1a** determined.

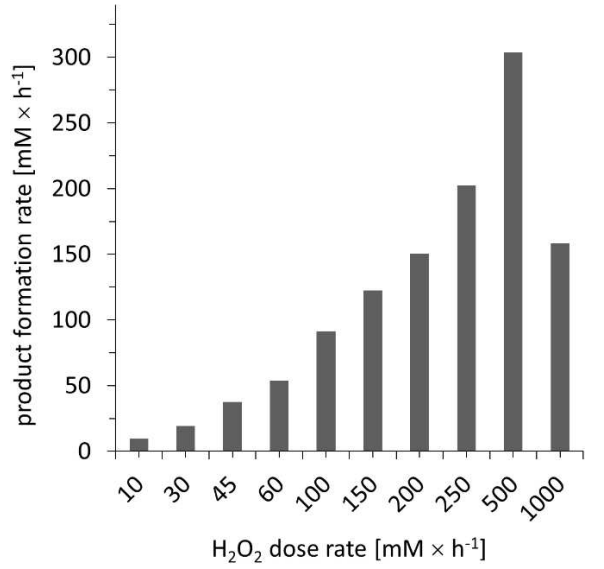

Figure 2. Influence of H_2O_2 addition rate on the rate of the conversion of **1a** to **1b**. Conditions: [**1a**] = 50 mM, [*Aae*UPO] = 1 μM, buffer: 50 mM KPi pH 7 containing 30% (v/v) of acetonitrile, 25 °C, 600 rpm. The reaction was initiated by addition of H_2O_2 (10–1000 mM h^{-1} from a 1 M stock). Please note, the abscissa is not linear.

ing dosage rate. The highest product formation rate observed in these experiments was 303 mM h^{-1} corresponding to a superb catalytic performance of *Aae*UPO of approx. 84 catalytic turnovers per second (ca. 109 U mg^{-1}). The slope in the linear region was around 0.78, indicating that approx. 22% of the H_2O_2 supplied was not used productively for product conversion. Most likely the known catalase activity of *Aae*UPO accounts for this observation.[11] Quite expectedly, further increase of the H_2O_2 addition rate resulted in a decrease of the overall reaction rate, which can be attributed to the irreversible, oxidative inactivation of the catalytic heme site of *Aae*UPO.[12]

With future preparative-scale applications in mind we further investigated the influence of starting material- and product-concentration on the activity of the biocatalyst (Figures S7 & S8). While the activity of *Aae*UPO was hardly influenced by concentrations of **1a** up to 500 mM, there seemed to be a mild inhibitory effect of the silanol product **2a** with *Aae*UPO activity steadily decreasing in the presence of increasing concentrations of **2a**. Under the current experimental conditions the volatility of the reagents, especially of **1a**, represented a challenge to achieve a closed mass balance (Figure S6). This, however, can be addressed in future experiments by using more suitable, gastight setups. To address the poor water solubility of most organosilane starting materials so-called two liquid phase systems (2LPSs) represent an attractive approach.[13] We therefore tested the feasibility of a 2LPS approach using **1a** as second, water immiscible phase serving as substrate reservoir and product sink (Figure S9) Already a preliminary experiment gave very promising results with linear product accumulation for at least 2 days and product concentrations (**2a**) of up to 121 mM, corresponding to more than 120000 catalytic turnovers of *Aae*UPO.

Encouraged by the promising results obtained with dimethylphenylsilane (**1a**), we further explored the scope of the *Aae*UPO-catalysed hydroxylation of organosilanes to several commercially available starting materials (Figure 3).

The majority of starting materials investigated was converted smoothly. Exceptions were the dihydrosilanes **1f** and **1g**, where significant background hydroxylation was observed in the absence of *Aae*UPO. We therefore did not attempt to determine the enantiomeric purity of the product **2f** also because it was not to be expected to be conformational stable under the current reaction conditions.[6a,14] In all other cases the control reactions yielded no detectable product formation (Figures S10–S111).

In case of the phenyl silanol products **2a**, **2c**, **2d**, **2e**, **2f** we observed additional products, which could be identified as silanol condensation products. We attribute their occurrence to the spontaneous condensation equilibrium of silanols in aqueous media[15] as also chemically produced silanols showed dimerisation tendencies in aqueous buffer (Figures S10–S111). Interestingly Arnold and co-workers explicitly mention the absence of any dimerisation products in their experiments. This apparent discrepancy with our observations may easily be explained by the significantly higher product concentrations achieved here and considering the concentration-dependency of the dimerisation equilibria.

Interestingly, for substrates **1j**, **1l** and **1m** the chemoselectivity of the hydroxylation was not exclusive and some (presumably) C–H hydroxylation byproducts were observed

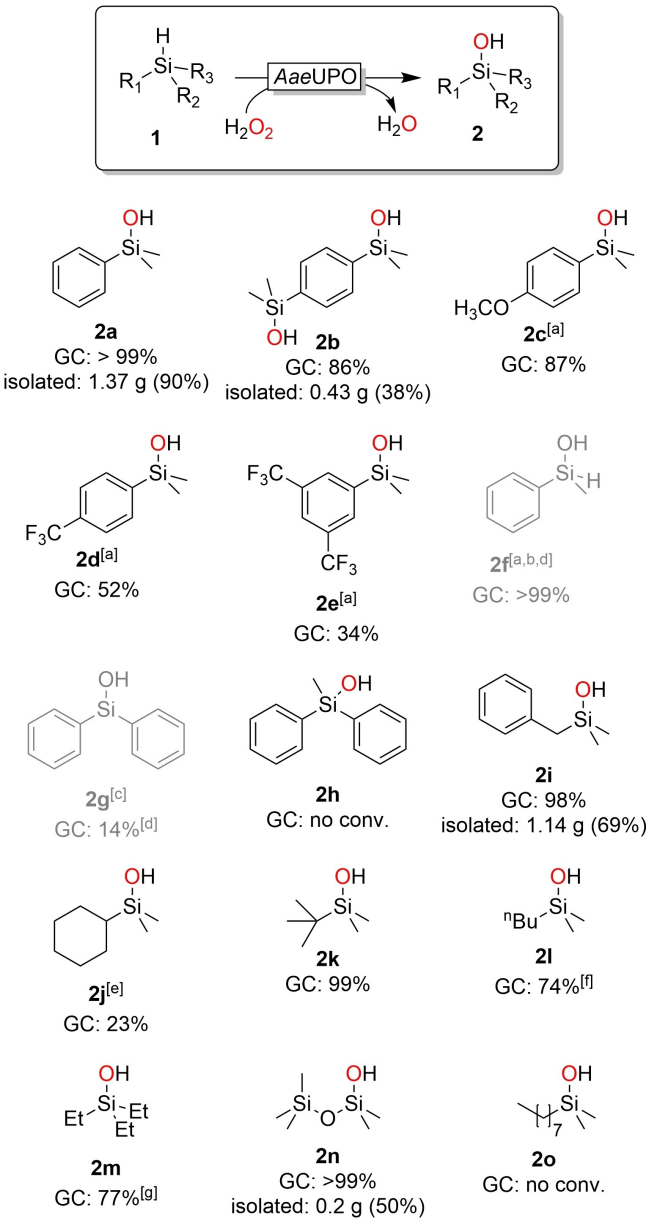

Figure 3. Substrate scope of *Aae*UPO-catalysed hydroxylation of organosilanes. General conditions: [Organosilane] = 50 mM, [*Aae*UPO] = 1 μM, buffer: 50 mM KPi pH 7.0 containing 30% (v/v) of acetonitrile, 25 °C, 600 rpm. The reaction was initiated by adding H_2O_2 (10 mM h^{-1} from a 1 M stock), 5 h. GC yields are given as averages of duplicate runs. For entries shown in grey, significant background conversion in the absence of *Aae*UPO was observed.[a]: significant amounts of dimerisation product observed; [b] negative controls showed approx. 45% conversion; [c] negative controls yielded the same conversion as in the presence of *Aae*UPO; [d] both, mono- and dihydroxylation products were observed: silanediol : silanol = 6 : 1; [e] approx. equal formation of a yet non characterised C–H hydroxylation product; [f] approx. 26% of a yet non characterised C–H hydroxylation product; [g] approx. 12% of a yet non characterised C–H hydroxylation product.

(Figures S78, 91 & 98). As pointed out by Arnold and coworkers, the lower Si–H bond dissociation energy (being roughly 10 kcal mol^{-1} lower than that of the C–H bonds[16]) should kinetically favour Si-hydroxylation over C-hydroxylation. Apparently, also the positioning of the starting material relative to the active compound I controls the regioselectivity of the *Aae*UPO-catalysed transformation.

To obtain further insights into the molecular basis for the selectivity of the *Aae*UPO-catalysed silane hydroxylation, Protein Energy Landscape Exploration (PELE) simulations[17] were performed. The distance between the heme compound I (Cpd I) oxygen and silicon-bound hydrogens (Figure 4 and Figure S2) were chosen as reactive coordinates. Simulations indicate that steric effects in both the channel and active site explain most selectivities observed in the enzymatic conversions. For instance, PELE simulations performed with dimethyl cyclohexyl silane (**1j**) revealed an almost equal distribution of productive poses exposing the Si–H and C_β–H bond to Cpd I (Figure 4), thereby qualitatively explaining the experimentally observed 1 : 1 ratio of Si–H to C–H hydroxylation. Similar trends were observed also for other substrates modelled (Figure S2).

Overall, PELE simulations qualitatively rationalise the chemoselectivity observed and will put the basis for future *Aae*UPO engineering to generate enzyme variants with tailored selectivity.

In summary, we have demonstrated that peroxygenases such as *Aae*UPO are promising catalysts for the oxyfunctionalisation of organosilanes. Compared to previously reported P450 monooxygenases[6a] the ease of application (simple direct use of H_2O_2 instead of sacrificial electron donors, molecular oxygen, and complex electron transport chains)[18] makes the UPO-based approach attractive. More significantly, *Aae*UPO provides noticeable catalytic turnovers (up to 120000) and turnover frequencies of up to 84 s^{-1}. Substrate induced-fit binding simulations provide a good understanding of the selectivity patterns, where steric hindrance was the major contributor.[19] This will put the basis for engineering *Aae*UPO variants[20] with improved activity and (enantio)selectivity towards sterically more demanding silanes for whose silanol products configurational stability of the enantiomers may be expected.[21]

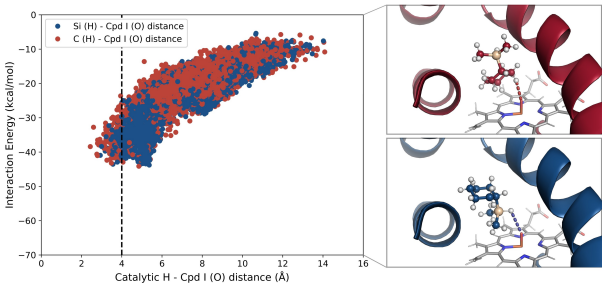

Figure 4. PELE simulation results for **1j** ligand. (Left) The scatter plot shows the sampled poses' catalytic distance between the reactive oxygen in Cpd I and the silicon (blue) or carbon (red) reactive hydrogens (only the shortest distance between these two atoms is shown) against the enzyme-substrate interaction energy. The vertical dashed line marks a threshold of 4 Å for the catalytic distance. (Right) Snapshots of the catalytic poses show the positioning of the substrate with a carbon- (right top) or silicon-reactive (right bottom) catalytic distance (dashed lines).

Acknowledgements

Funded by the European Union (ERC, PeroxyZyme, No 101054658). Views and opinions expressed are however those of the authors only and do not necessarily reflect those of the European Union or the European Research Council. Neither the European Union nor the granting authority can be held responsible for them. X.X. thanks the Guangzhou Elite Project for a fellowship. S.R. thanks the Spanish Ministry of Science and Innovation for a PhD fellowship (FPU19/00608). Modelling work was financed by the PID2019-106370RB-I00 grant from the Spanish Ministry of Science and Innovation. We thank Stephen Eustace, Lloyd Mallée, and Marc Strampraad for technical support.

Conflict of Interest

The authors declare no conflict of interest.

Data Availability Statement

The data that support the findings of this study are available in the Supporting Information of this article.

Keywords: Biocatalysis · Oxyfunctionalization · PELE Simulations · Peroxygenase · Silanols

[1] a) M. Jeon, J. Han, J. Park, *ACS Catal.* **2012**, *2*, 1539–1549; b) V. Chandrasekhar, R. Boomishankar, S. Nagendran, *Chem. Rev.* **2004**, *104*, 5847–5910.

[2] J. A. Cella, J. C. Carpenter, *J. Organomet. Chem.* **1994**, *480*, 23–26.

[3] a) G. H. Barnes, N. E. Daughenbaugh, *J. Org. Chem.* **1966**, *31*, 885–887; b) M. Lee, S. Ko, S. Chang, *J. Am. Chem. Soc.* **2000**, *122*, 12011–12012; c) M. Shi, K. M. Nicholas, *J. Chem. Res.* **1997**, 400–401; d) M. Yu, H. Jing, X. Liu, X. Fu, *Organometallics* **2015**, *34*, 5754–5758; e) Y. Kikukawa, Y. Kuroda, K. Yamaguchi, N. Mizuno, *Angew. Chem. Int. Ed.* **2012**, *51*, 2434–2437; f) E. A. Ison, R. A. Corbin, M. M. Abu-Omar, *J. Am. Chem. Soc.* **2005**, *127*, 11938–11939; g) E. Matarasso-Tchiroukhine, *J. Chem. Soc. Chem. Commun.* **1990**, 681–682; h) U. Schubert, C. Lorenz, *Inorg. Chem.* **1997**, *36*, 1258–1259; i) A. K. Liang Teo, W. Y. Fan, *Chem. Commun.* **2014**, *50*, 7191–7194.

[4] a) Y. Okada, M. Oba, A. Arai, K. Tanaka, K. Nishiyama, W. Ando, *Inorg. Chem.* **2010**, *49*, 383–385; b) A. V. Arzumanyan, I. K. Goncharova, R. A. Novikov, S. A. Milenin, K. L. Boldyrev, P. N. Solyev, Y. V. Tkachev, A. D. Volodin, A. F. Smol'yakov, A. A. Korlyukov, A. M. Muzafarov, *Green Chem.* **2018**, *20*, 1467–1471; c) H. Li, L. Chen, P. Duan, W. Zhang, *ACS Sustainable Chem. Eng.* **2022**, *10*, 4642–4649.

[5] a) W. Adam, C. M. Mitchell, C. R. Saha-Möller, O. Weichold, H. Garcia, *Chem. Commun.* **1998**, 2609–2610; b) D. Limnios, C. G. Kokotos, *ACS Catal.* **2013**, *3*, 2239–2243; c) A. T. Kelly, A. K. Franz, *ACS Omega* **2019**, *4*, 6295–6300; d) K. Wang, J. Zhou, Y. Jiang, M. Zhang, C. Wang, D. Xue, W. Tang, H. Sun, J. Xiao, C. Li, *Angew. Chem. Int. Ed.* **2019**, *58*, 6380–6384.

[6] a) S. Bähr, S. Brinkmann-Chen, M. Garcia-Borras, J. M. Roberts, D. E. Katsoulis, K. N. Houk, F. H. Arnold, *Angew. Chem. Int. Ed.* **2020**, *59*, 15507–15511; b) S. B. J. Kan, R. D. Lewis, K. Chen, F. H. Arnold, *Science* **2016**, *354*, 1048–1051; c) R. J. Fessenden, R. A. Hartman, *J. Med. Chem.* **1970**, *13*, 52–54.

[7] a) H. Nishino, T. Mori, Y. Okahata, *Chem. Commun.* **2002**, *22*, 2684–2685; b) P. B. Brondani, M. Mittersteiner, M. A. Voigt, B. H. Klinkowski, D. Riva Scharf, P. C. De Jesus, *Synthesis* **2019**, *51*, 477–485; c) A. R. Bassindale, K. F. Brandstadt, T. H. Lane, P. G. Taylor, *J. Inorg. Biochem.* **2003**, *96*, 401–406; d) N. Kröger, S. Lorenz, E. Brunner, M. Sumper, *Science* **2002**, *298*, 584–586; e) A. R. Bassindale, K. F. Brandstadt, T. H. Lane, P. G. Taylor in *Polymer Biocatalysis and Biomaterials, Vol. 900*, American Chemical Society, **2005**, pp. 164–181.

[8] a) R. Ullrich, J. Nüske, K. Scheibner, J. Spantzel, M. Hofrichter, *Appl. Environ. Microbiol.* **2004**, *70*, 4575–4581; b) F. Tonin, F. Tieves, S. Willot, A. Van Troost, R. Van Oosten, S. Breestraat, S. van Pelt, M. Alcalde, F. Hollmann, *Org. Process Res. Dev.* **2021**, *25*, 1414–1418; c) P. Molina-Espeja, S. Ma, D. M. Mate, R. Ludwig, M. Alcalde, *Enzyme Microb. Technol.* **2015**, *73–74*, 29–33; d) P. Molina-Espeja, E. Garcia-Ruiz, D. Gonzalez-Perez, R. Ullrich, M. Hofrichter, M. Alcalde, *Appl. Environ. Microbiol.* **2014**, *80*, 3496–3507.

[9] M. Hobisch, D. Holtmann, P. G. de Santos, M. Alcalde, F. Hollmann, S. Kara, *Biotechnol. Adv.* **2021**, *51*, 107615.

[10] T. Hilberath, A. van Troost, M. Alcalde, F. Hollmann, *Front. Catal.* **2022**, *2*, 882992.

[11] M. Hofrichter, R. Ullrich, *Appl. Microbiol. Biotechnol.* **2006**, *71*, 276–288.

[12] B. O. O. Burek, S. Bormann, F. Hollmann, J. Bloh, D. Holtmann, *Green Chem.* **2019**, *21*, 3232–3249.

[13] M. Van Schie, J.-D. Spöring, M. Bocola, P. Dominguez de Maria, D. Rother, *Green Chem.* **2021**, *23*, 3191–3206.

[14] a) R. J. P. Corriu, C. Guerin, *J. Organomet. Chem.* **1980**, *198*, 231–320; b) C. Chuit, R. J. P. Corriu, C. Reye, J. C. Young, *Chem. Rev.* **1993**, *93*, 1371–1448.

[15] a) W. T. Grubb, *J. Am. Chem. Soc.* **1954**, *76*, 3408–3414; b) C. J. Brinker, *J. Non-Cryst. Solids* **1988**, *100*, 31–50.

[16] R. Walsh, *Acc. Chem. Res.* **1981**, *14*, 246–252.

[17] S. Acebes, E. Fernandez-Fueyo, E. Monza, M. F. Lucas, D. Almendral, F. J. Ruiz-Dueñas, H. Lund, A. T. Martinez, V. Guallar, *ACS Catal.* **2016**, *6*, 1624–1629.

[18] D. Holtmann, F. Hollmann, *ChemBioChem* **2016**, *17*, 1391–1398.

[19] a) G. Qu, A. Li, C. G. Acevedo-Rocha, Z. Sun, M. T. Reetz, *Angew. Chem. Int. Ed.* **2020**, *59*, 13204–13231; b) G.-D. Roiban, M. T. Reetz, *Chem. Commun.* **2015**, *51*, 2208–2224; c) F. H. Arnold, *Angew. Chem. Int. Ed.* **2018**, *57*, 4143–4148.

[20] P. Gomez de Santos, I. Mateljak, M. D. Hoang, S. J. Fleishman, F. Hollmann, M. Alcalde, *J. Am. Chem. Soc.* **2023**, *145*, 3443–3453.

[21] W. Yuan, X. Zhu, Y. Xu, C. He, *Angew. Chem. Int. Ed.* **2022**, *61*, e202204912.

Manuscript received: February 24, 2023
Accepted manuscript online: April 6, 2023
Version of record online: ■■, ■■

Communications

Biocatalysis

X. Xu, J. M. A. van Hengst, Y. Mao, M. Martinez, S. Roda, M. Floor, V. Guallar, C. E. Paul, M. Alcalde, F. Hollmann* ——— **e202302844**

Peroxygenase-Catalysed Selective Oxidation of Silanes to Silanols

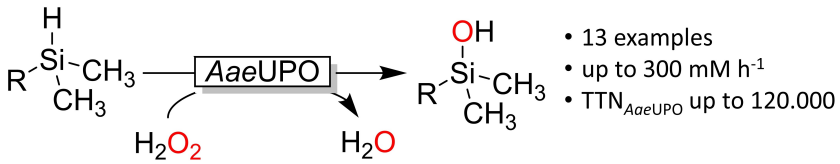

The peroxygenase from *Agrocybe aegerita* (*Aae*UPO) efficiently hydroxylates organosilanes to the corresponding silanols. The methodology proposed here excels by its simplicity and high productivity. Protein Energy Landscape Exploration (PELE) simulations provide a rationale for the selectivities observed and put the basis for future *Aae*UPO engineering.